

Spectroscopic Characterization of Molybdenum Dinitrogen Complexes Containing a Combination of Di- and Triphosphine Coligands: ^{31}P NMR Analysis of Five-Spin Systems

Kristina Klatt, Gerald Stephan, Gerhard Peters, and Felix Tuczek*

Institut für Anorganische Chemie, Christian Albrechts Universität Kiel, Otto Hahn Platz 6/7, D-24098 Kiel, Germany

Received February 29, 2008

The three molybdenum- N_2 complexes $[\text{Mo}(\text{N}_2)(\text{dpepp})(\text{depe})]$ (**1**), $[\text{Mo}(\text{N}_2)(\text{dpepp})(\text{dppe})]$ (**2**), and $[\text{Mo}(\text{N}_2)(\text{dpepp})(1,2\text{-dppp})]$ (**3**), all of which contain a combination of a bi- and a tridentate phosphine ligand, were prepared and investigated by vibrational and ^{31}P NMR spectroscopy. As a tridentate ligand bis(2-diphenylphosphinoethyl)phenylphosphine (dpepp) has been employed. The three different bidentate ligands are 1,2-bis(diethylphosphino)ethane (depe), 1,2-bis(diphenylphosphino)ethane (dppe), and R-(+)-1,2-bis(diphenylphosphino)propane (1,2-dppp). N–N as well as metal–N vibrations of **1–3** are identified and interpreted in terms of the geometric and electronic structures of the complexes. ^{31}P NMR spectra are recorded and fully analyzed. Moreover, correlation spectroscopy (COSY)-45 measurements are performed to determine the relative signs of coupling constants. Special attention is directed to a detection of different isomers and their ^{31}P NMR, as well as vibrational spectroscopic properties. The implications of the results for the area of synthetic nitrogen fixation with phosphine complexes are discussed.

1. Introduction

^{31}P NMR spectroscopy has proven to be a valuable tool for the elucidation of the solution structure of transition-metal phosphine complexes.¹ This class of compounds has also been of significant interest with respect to synthetic nitrogen fixation. As demonstrated by the groups of Chatt, Hidai, and others, molybdenum and tungsten dinitrogen complexes of the type $[\text{M}(\text{N}_2)_2(\text{monophos})_4]$ or $[\text{M}(\text{N}_2)_2(\text{diphos})_2]$ can be protonated at the N_2 ligand to ultimately give NH_3 (monophos = PR_3 , R = Me, Ph; diphos = $\text{Ph}_2\text{PCH}_2\text{CH}_2\text{PPh}_2$ (dppe) and $\text{Et}_2\text{PCH}_2\text{CH}_2\text{PEt}_2$ (depe)).² For the diphos systems, many complex-bound intermediates of the reduction and protonation of N_2 have been isolated and characterized, respectively, making these compounds func-

tional models of the enzyme nitrogenase.³ Despite an early success with respect to a cyclic conversion of N_2 to NH_3 ,⁴ however, no truly catalytic action could be achieved on the basis of this chemistry (“Chatt cycle”) so far. This is in contrast to the recently synthesized Mo(III) triamidoamine complex containing sterically demanding residues for which a catalytic generation of ammonia from N_2 has been demonstrated (Schrock cycle).⁵

To obtain information on the energetics of the Chatt cycle, we have recently treated all involved intermediates, the employed acid as well as the reductant, with density-functional theory (DFT) and have determined the free

* To whom correspondence should be addressed. E-mail: ftuczek@ac.uni-kiel.de.

- (1) (a) Henry, R. M.; Shoemaker, R. K.; Newell, R. H.; Jacobsen, G. M.; DuBois, D. L.; Rakowski DuBois, M. *Organometallics* **2005**, *24*, 2481. (b) Pregosin, P. S.; Kunz, R. W., *NMR Basic Principles and Progress*; Springer Verlag: New York, 1979; Vol. 16. (c) Verkade, J. G. *Coord. Chem. Rev.* **1972**, *9*, 1.
- (2) (a) MacKay, B. A.; Fryzuk, M. D. *Chem. Rev.* **2004**, *104*, 385. (b) Hidai, M.; Mizobe, Y. *Chem. Rev.* **1995**, *95*, 1115. (c) Henderson, R. A.; Leigh, G. J.; Pickett, C. J. *Adv. Inorg. Chem. Radiochem.* **1983**, *27*, 197. (d) Chatt, J.; Dilworth, J. R.; Richards, R. L. *Chem. Rev.* **1978**, *78*, 589.

- (3) (a) *Prokaryotic Nitrogen Fixation: A Model System for the Analysis of a Biological Process*; Triplett, E. W., Ed.; Horizon Scientific Press: Norfolk, U.K., 2000. (b) Burgess, B. K.; Lowe, D. J. *Chem. Rev.* **1996**, *96*, 2983.
- (4) (a) Pickett, C. J.; Talarmin, J. *Nature* **1985**, *317*, 652. (b) Pickett, C. J.; Ryder, K. S.; Talarmin, J. J. C. S. *Dalton Trans., Inorg. Chem.* **1986**, *7*, 1453.
- (5) (a) Yandulov, D. V.; Schrock, R. R. *J. Am. Chem. Soc.* **2002**, *124*, 6252. (b) Yandulov, D. V.; Schrock, R. R.; Rheingold, A. L.; Ceccarelli, C.; Davis, W. M. *Inorg. Chem.* **2003**, *42*, 796. (c) Yandulov, D. V.; Schrock, R. R. *Science* **2003**, *301*, 76. (d) Ritleng, V.; Yandulov, D. V.; Weare, W. W.; Schrock, R. R.; Hock, A. S.; Davis, W. M. *J. Am. Chem. Soc.* **2004**, *126*, 6150. (e) Yandulov, D. V.; Schrock, R. R. *Inorg. Chem.* **2005**, *44*, 1103. (f) Yandulov, D. V.; Schrock, R. R. *Inorg. Chem.* **2005**, *44*, 5542. (g) Yandulov, D. V.; Schrock, R. R. *Can. J. Chem.* **2005**, *83*, 341.

reaction enthalpies for all protonation and reduction reactions.⁶ As in our previous DFT study of the Schrock cycle,⁷ decamethylchromocene was employed as reductant. For the protonation reactions, two acids were considered, HBF₄/diethylether and a lutidinium salt. For all protonation and reduction steps, the corresponding free reaction enthalpy changes were calculated. The derived energy profile and corresponding reaction mechanism bear strong similarities to the Schrock cycle. For HBF₄/diethylether as acid and Cp*₂Cr as reductant, a catalytic cycle consisting of thermally allowed reactions was predicted. However, this cycle involves a Mo(I) fluoro complex as dinitrogen intermediate which is unstable toward disproportionation. If a truly catalytic action of the Chatt system is intended, strategies have to be developed to avoid disproportionation of the Mo(I) dinitrogen complex to a Mo(II) complex carrying two anionic ligands. Important points in this respect are (i) avoiding the presence of strongly Lewis-basic species (such as F⁻) in solution and (ii) employing multidentate ligands with more than two P-donors that also occupy the *trans*-position of coordinated N₂, in contrast to the conventional Chatt-type Mo and W diphosphine systems.

The only existing phosphine-coordinated molybdenum dinitrogen complexes which meet the second criterion have been prepared by George et al. using a combination of a diphosphine and a triphosphine ligand.⁸ In analogy to the Mo triamidoamine complexes, these systems exhibit only one binding site for N₂ and can be protonated to give NNH₂ complexes. In a previous study, we investigated the electronic structure and the spectroscopic properties of the complex [Mo(N₂)(dpepp)(dppm)] (dpepp = bis(diphenylphosphinoethyl)phenylphosphine, PhP(CH₂CH₂PPh₂)₂; dppm = bis(diphenylphosphino)methane, Ph₂PCH₂PPh₂) and its hydrazido(2-) derivative.⁹ ¹⁵N- and ³¹P NMR spectroscopic data were presented and analyzed with the help of spectral simulations. Moreover, infrared (IR) and Raman spectra were recorded and evaluated using a quantum chemistry based normal coordinate analysis (QCB-NCA). The spectroscopic results were interpreted with the help of DFT calculations. These studies showed that the activation of the N₂ ligand of the parent N₂ complex is *lower* than in the *trans*-acetonitrile complex [Mo(N₂)(NCCH₃)(dppe)₂], but *higher* than in the bis(dinitrogen) complex [Mo(N₂)₂(dppe)₂]. This was interpreted in terms of the relative σ/π-donor and π-acceptor capabilities of the respective *trans*-ligands. More recently, we also applied our DFT analysis to the cyclic reduction and protonation of N₂ mediated by this complex and found

that a catalytic ammonia synthesis from N₂ should in fact be thermodynamically feasible if the phosphine ligands remain coordinated to the metal center.¹⁰

Herein we present spectroscopic investigations on molybdenum dinitrogen complexes containing a combination of dpepp with diphos ligands exhibiting C₂ bridges, that is, depe, dppe, and R-(+)-1,2-dppp (Ph₂PC*H(CH₃)CH₂PPh₂). Specifically, the three compounds [Mo(N₂)(dpepp)(depe)] (**1**), [Mo(N₂)(dpepp)(dppe)] (**2**), and [Mo(N₂)(dpepp)(1,2-dppp)] (**3**) were prepared and investigated by vibrational and ³¹P NMR spectroscopy. Complex **1** was found to exist in only one form. Compound **2** had already been synthesized by George et al.⁸ In agreement with these authors, we identified two isomers, [Mo(N₂)(dpepp)(dppe)] (**2a**) and *iso*-[Mo(N₂)(dpepp)(dppe)] (**2b**). For compound **3** evidence for the existence of two diastereomers (isomer **A** and **B**, **3a** and **3b**) was obtained as well. In this case, however, the isomerism is not induced by the coordination geometry of the complex but by an optically active ligand. In the present paper particular emphasis is put on the one- and two-dimensional ³¹P NMR spectroscopic characterization of complexes **1–3** in solution, as well as on a full analysis of the corresponding five-spin systems. Moreover, IR and Raman spectra of these complexes are recorded and correlated with the NMR-spectroscopic information. The implications of the results with respect to synthetic nitrogen fixation are discussed.

2. Experimental Section

Synthesis and Sample Preparation. All reactions were carried out under an N₂-atmosphere by using Schlenk-techniques. Solvents were dried and freshly distilled under argon. All other reagents were used in the available qualities. The phosphine ligands were obtained from Strem Chemicals. The preparations were performed according to the literature⁸ with slight modifications.

[Mo(N₂)(dpepp)(depe)] (1**).** This synthesis was carried out as described for **2** (see below) by using sodium amalgam (200 mg Na, 30.0 g Hg), 450 mg of (0.58 mmol) [MoCl₃(dpepp)], 140 mg of (0.68 mmol) depe, and 20 mL of THF. Elemental Anal. Calcd: C, 61.1; H, 6.6; N, 3.2. Found: C, 61.0; H, 6.9; N, 2.6. ³¹P{¹H} = δ_{31P} = 87.25 ppm (dddd, ²J_{ea/eb} = -15.5 Hz, ^{1/2}³J_{ed/ec} = 4.7 Hz, P_e), 62.12 ppm (dddd, ²J_{cd} = -9.5 Hz, ²J_{ac/bd} = -18.6 Hz, ²J_{ad/bc} = 98.3 Hz, P_{c/d}), 48.80 ppm (dddd, ^{2/3}J_{ab} = -4.9 Hz, P_{a/b}).

[Mo(N₂)(dpepp)(dppe)] (2**).** A suspension of 570 mg of (0.74 mmol) [MoCl₃(dpepp)] and 350 mg of (0.87 mmol) dppe in 20 mL of THF was added to sodium amalgam (200 mg Na, 30.0 g Hg) and stirred for 3 h at 0 °C and 16 h at ambient temperature under N₂. The solution was decanted, filtered and reduced in vacuo to 6 mL. Six milliliters of methanol were added, and the solution was reduced again. After addition again of 6 mL of methanol, the formed precipitate was filtered off, washed with 4 × 4 mL methanol, and dried in vacuo. Elemental Anal. Calcd: C, 68.1; H, 5.4; N, 2.6. Found: C, 67.9; H, 5.6; N, 2.2. **2a**: ³¹P{¹H} = δ_{31P} = 73.80 (quin; P_e), 63.40 (d; P_{a,b,c,d}) ppm. **2b**: ³¹P{¹H} = δ_{31P} = 90.94 (ddd, ²J_{ea} = 106.7 Hz, ²J_{eb} = -16.6 Hz, ^{2/3}J_{ec} = 7.2 Hz, ^{2/3}J_{ed} = 1.5 Hz; P_e), 72.30 (dddd, ²J_{cb} = 101.6 Hz, ²J_{ca} = -21.2 Hz, ²J_{cd} =

(6) Stephan, G.; Sivasankar, Ch.; Tuczek, F. *Chem. Eur. J.* **2008**, *14*, 644–652.

(7) Studt, F.; Tuczek, F. *Angew. Chem., Int. Ed.* **2005**, *44*, 5639–5642.

(8) (a) George, T. A.; Tisdale, R. C. *Inorg. Chem.* **1988**, *27*, 2909. (b) George, T. A.; Tisdale, R. C. *J. Am. Chem. Soc.* **1985**, *107*, 5157. (c) George, T. A.; Ma, L.; Shailh, S. N.; Tisdale, R. C.; Zubieta, J. *Inorg. Chem.* **1990**, *29*, 4789.

(9) Stephan, G. C.; Peters, G.; Lehnert, N.; Habeck, C. M.; Näther, C.; Tuczek, F. *Can. J. Chem.* **2005**, *83*, 385.

(10) Stephan, G.; Tuczek, F. In *Activating Unreactive Substrates*; Bolm, C.; Hahn, E., Eds.; Wiley VCH: New York, 2008; submitted for publication.

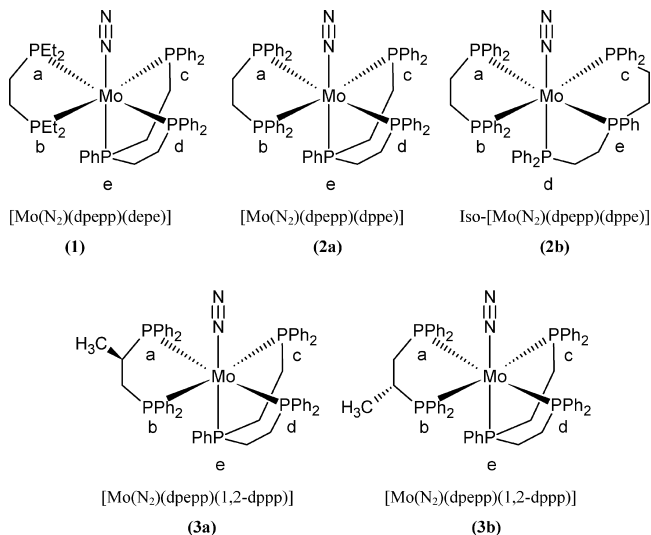


Figure 1. Synthesized complexes.

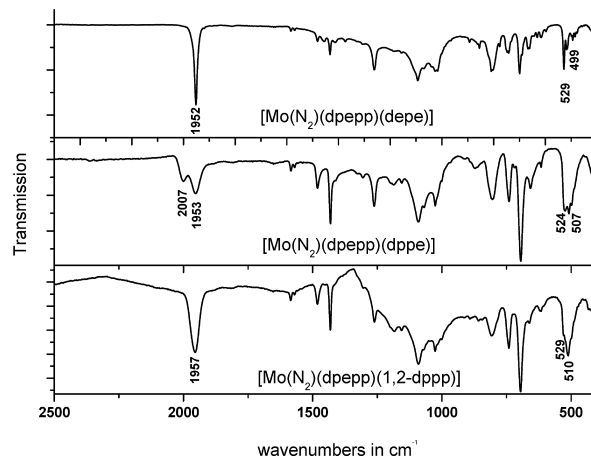
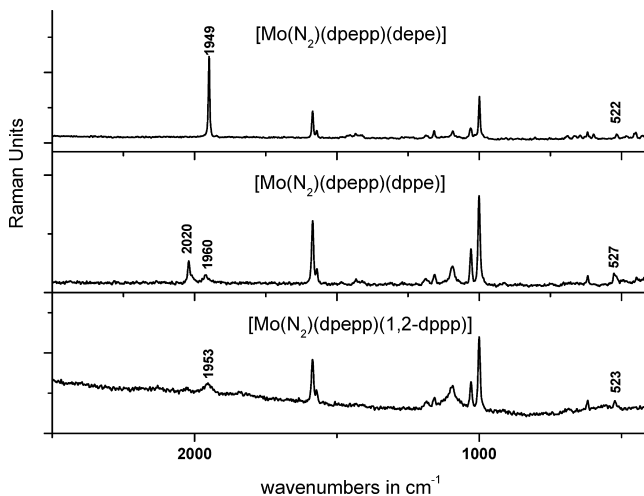
−13.1 Hz; P_c), 69.10 (dddd, $^2J_{bc} = 101.6$ Hz, $^{2/3}J_{ba} = 5.1$ Hz, $^2J_{bd} = -9.7$ Hz; P_b), 67.00 (ddt; P_a), 61.10 (ddd; P_d) ppm.

$[\text{Mo}(\text{N}_2)(\text{dpepp})(1,2\text{-dppp})]$ (3). This synthesis was performed in analogy to that of **2** by using sodium amalgam (200 mg Na, 30.0 g Hg), 419 mg of (0.540 mmol) $[\text{MoCl}_3(\text{dpepp})]$, 265 mg of (0.640 mmol) 1,2-dppp, and 20 mL of THF. Elemental Anal. Calcd: C, 69.1; H, 5.4; N, 2.6. Found: C, 68.9; H, 5.7; N, 2.1. **3a:** $^{31}\text{P}\{^1\text{H}\} = \delta_{31\text{P}} = 71.90$ (dd, $^2J_{ea} = -10.6$ Hz, $^2J_{eb} = -15.1$ Hz, $^{2/3}J_{ec} = 1.5$ Hz, $^{2/3}J_{ed} = -1.5$ Hz; P_c), 69.81 (ddd, $^2J_{ad} = 99.2$ Hz, $^2J_{bd} = -25.1$ Hz, $^2J_{cd} = -4.1$ Hz, $^{2/3}J_{de} = -1.5$ Hz; P_d), 62.15 (dddd, $^2J_{ad} = 99.2$ Hz, $^2J_{ae} = -10.6$ Hz, $^2J_{ac} = -21.0$ Hz, $^{2/3}J_{ab} = -6.6$ Hz; P_a), 58.40 (dddd, $^2J_{bc} = 98.0$ Hz, $^2J_{be} = -15.1$ Hz, $^2J_{bd} = -25.1$ Hz, $^{2/3}J_{ba} = -6.6$ Hz; P_b), 55.90 (ddd, $^2J_{cb} = 98.0$ Hz, $^2J_{ca} = -21.0$ Hz, $^2J_{cd} = -4.1$ Hz, $^{2/3}J_{ce} = 1.5$ Hz; P_c) ppm. **3b:** $^{31}\text{P}\{^1\text{H}\} = \delta_{31\text{P}} = 77.76$ (dddd, $^2J_{bc} = 100.3$ Hz, $^2J_{bd} = -24.4$ Hz, $^2J_{be} = -15.8$ Hz, $^{2/3}J_{ba} = -8.2$ Hz; P_b), 72.50 (ddd, $^2J_{da} = 98.7$ Hz, $^2J_{db} = -24.4$ Hz, $^2J_{dc} = -3.2$ Hz, $^{2/3}J_{de} = -1.5$ Hz; P_d), 71.02 (dd, $^2J_{eb} = -15.8$ Hz, $^2J_{ea} = -10.8$ Hz, $^{2/3}J_{ec} = 1.5$ Hz, $^{2/3}J_{ed} = -1.5$ Hz; P_e), 56.60 (ddd, $^2J_{cb} = 100.3$ Hz, $^2J_{ca} = -22.8$ Hz, $^2J_{cd} = -3.2$ Hz, $^{2/3}J_{ce} = 1.5$ Hz; P_c), 43.17 (dddd, $^2J_{ad} = 98.7$ Hz, $^2J_{ac} = -22.8$ Hz, $^2J_{ae} = -10.8$ Hz, $^{2/3}J_{ab} = -8.2$ Hz; P_a) ppm.

Spectroscopic Characterization. Infrared spectra of the solid compounds were obtained from KBr pellets using a Bruker IFS v66/S FT-IR spectrometer. The FT Raman spectra were recorded with a Bruker IFS 666/CS NIR FT-Raman spectrometer at RT. As lightsource a NdYAG-Laser with an excitation wavelength of 1064 nm was used. The samples which absorbed at this wavelength were measured with 15% intensity. NMR spectra were measured with a Bruker AVANCE 400 Puls Fourier Transform spectrometer operating with a ^1H frequency of 400.13 MHz and a ^{31}P frequency of 161.98 MHz using a 5 mm inverse triple-resonance probe head. Referencing was done with TMS $\delta_{\text{H}} = 0$ ppm and 85% pure H_3PO_4 $\delta_{31\text{P}} = 0$ ppm as substitutive standards. All samples were measured in $\text{THF-}d_8$ at 300 K. All ^{31}P NMR spectra have been recorded with ^1H composite pulse decoupling. Simulated spectra were created with the program MESTREC.¹¹

3. Results and Analysis

Schematic structures of the complexes synthesized and investigated in this study are given in Figure 1. IR spectra

Figure 2. IR spectra of **1** (top), **2** (middle), and **3** (bottom) measured in KBr.Figure 3. Raman spectra of complexes **1**(top), **2** (middle), and **3** (bottom) measured as pure solids.Table 1. Vibrational Data of Complexes **1–3**

vibration	$[\text{Mo}(\text{N}_2)(\text{dpepp})(\text{depe})]$ 1	$[\text{Mo}(\text{N}_2)(\text{dpepp})(\text{dppe})]$ 2	$[\text{Mo}(\text{N}_2)(\text{dpepp})(1,2\text{-dppp})]$ 3
$\nu(\text{NN})$	1952 IR 1949 Raman	2007/1953 IR 2020/1960 Raman	1957 IR 1953 Raman
$\nu(\text{MoN})$	~ 450 (IR, Raman)		
$\delta(\text{MoNN})$	499, 493 (IR)	507, 497 (IR)	510, ~ 500 (IR)

of complexes **1–3** are displayed in Figure 2; the corresponding Raman spectra are shown in Figure 3. By comparison with the spectra of $[\text{Mo}(\text{N}_2)(\text{dpepp})(\text{dppm})]$ for which a ^{15}N substitution has been performed it is possible to identify the N–N– and metal–N vibrations of the three complexes (cf. Table 1).⁹ ^{31}P NMR spectra of **1–3** are displayed in Figures 4–6; the corresponding parameters are collected in Table 2. For compounds **2** and **3**, ^{31}P – ^{31}P -COSY-45(^1H CPD) measurements were performed. Assuming that the *trans*-coupling constant is positive, the absolute signs of the coupling constants were determined. Because of the similar geometry, the signs obtained from the analysis of the COSY-45 spectra of compound **3** were also adapted to compound **1**. The resulting coupling constants are shown in Scheme 1. Detailed analyses of the spectra are presented in the following, with particular emphasis on the identification of the different isomers.

(11) Mestrec, Mestrelab Research, Santiago de Compostela.

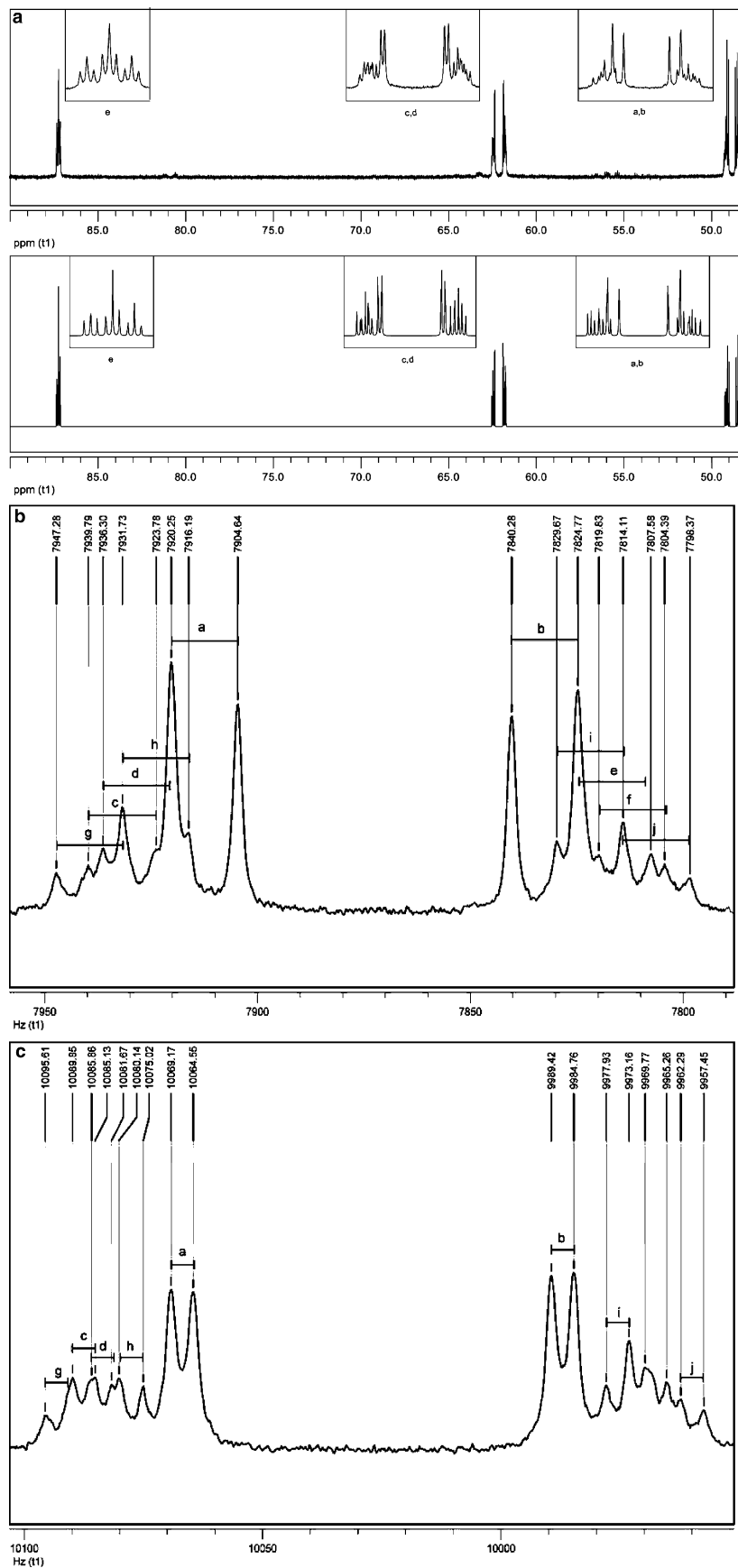


Figure 4. (a) $^{31}\text{P}\{^1\text{H}\}$ -NMR (161.98 MHz, in THF-d_8) of $[\text{Mo}(\text{N}_2)(\text{dpepp})(\text{depe})]$ (**1**), measured (top) and simulated (bottom); (b) M-Spectrum of **1**, expansion of the signal at 48.80 ppm; (c) X-Spectrum of **1**, expansion of the signal at 62.12 ppm.

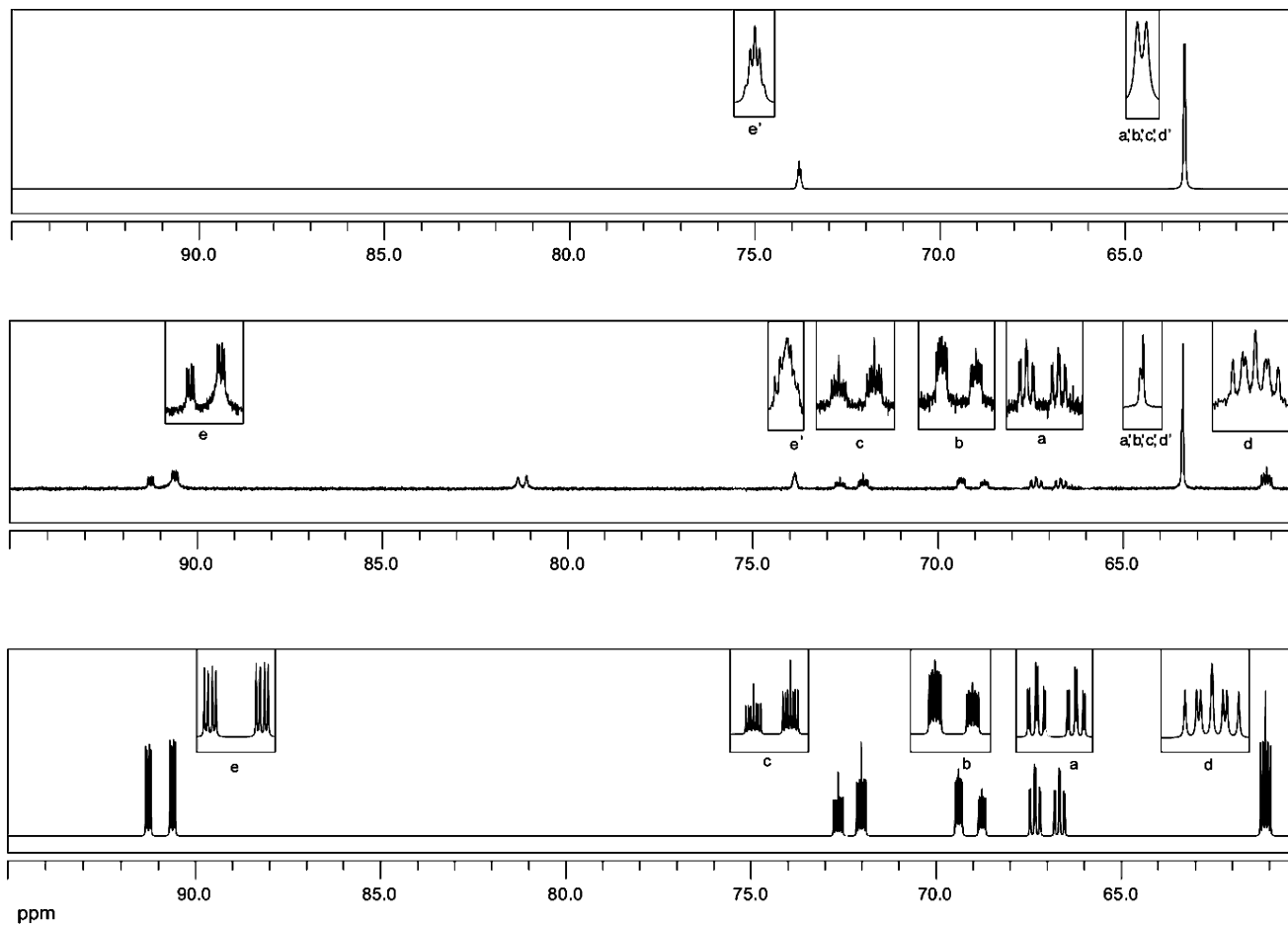


Figure 5. $^{31}\text{P}\{^1\text{H}\}$ -NMR (161.98 MHz, in $\text{THF-}d_8$) of $[\text{Mo}(\text{N}_2)(\text{dpepp})(\text{dppe})]$ (2), measured and simulated.

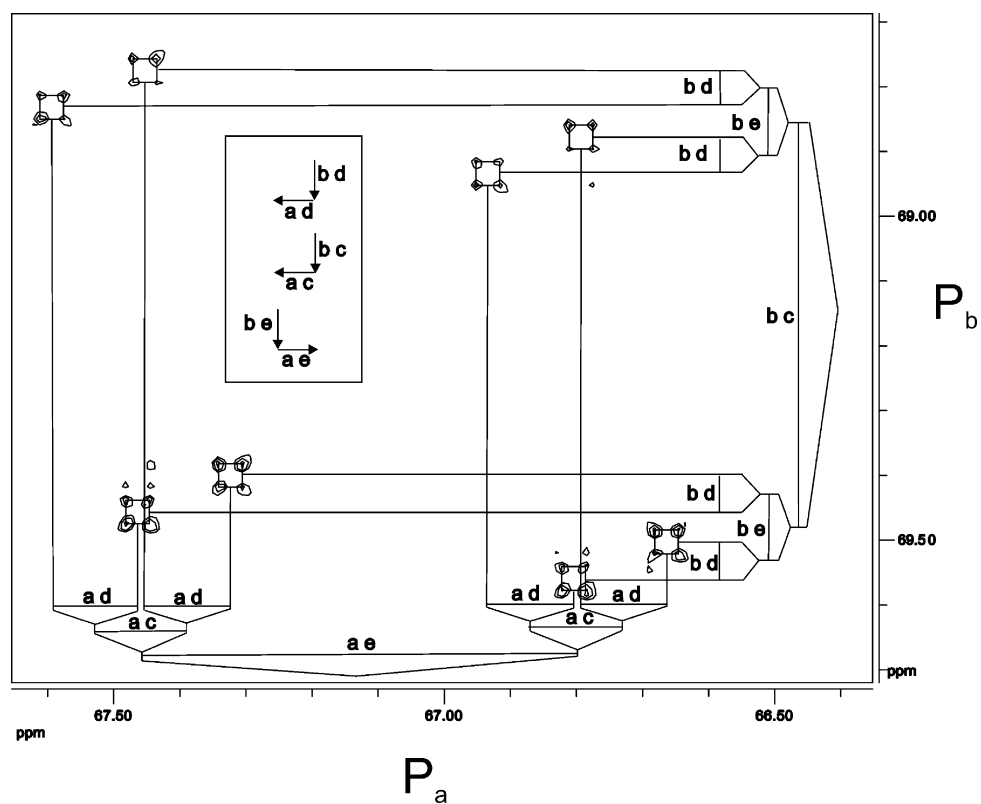
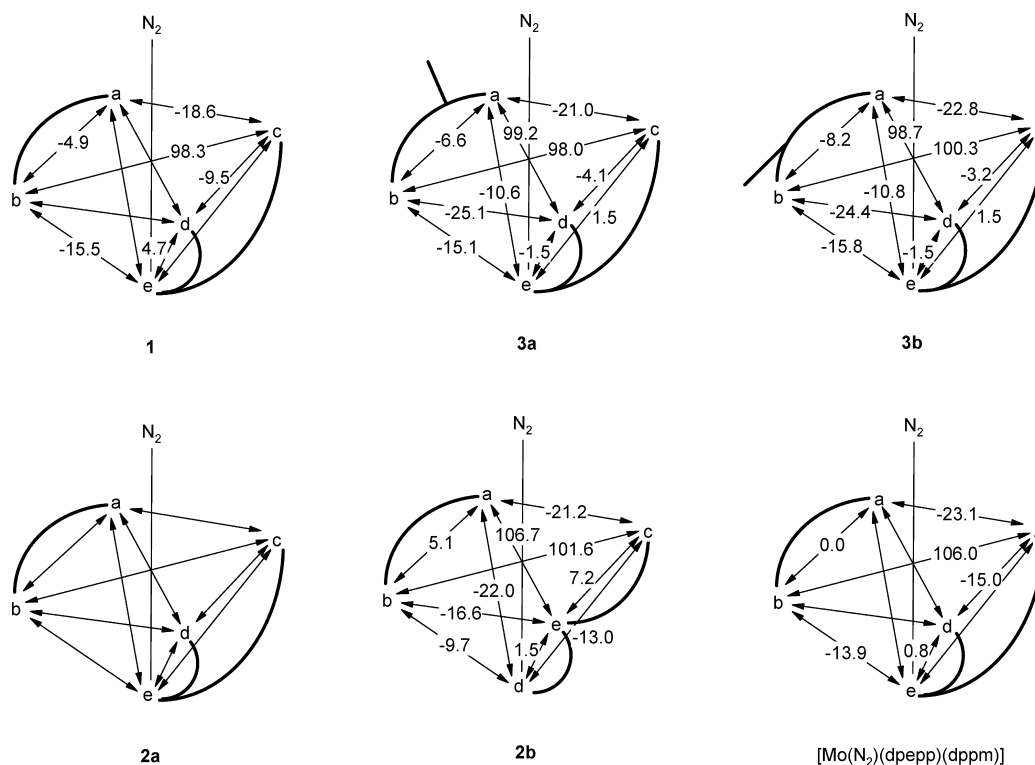


Figure 6. Expansion of the crosspeak P_a/P_b (67.00 ppm/69.10 ppm) of $[\text{Mo}(\text{N}_2)(\text{dpepp})(\text{dppe})]$ (2, COSY-45, 161.98 MHz, in $\text{THF-}d_8$).

Table 2. ^{31}P NMR Data of Complexes **1**–**3**

[Mo(N ₂)(dpepp)(depe)] 1		[Mo(N ₂)(dpepp)(dppe)] 2a		Iso-[Mo(N ₂)(dpepp)(dppe)] 2b	
P _{a/b} δ = 48.80 ppm	$^2J_{ad/bc}$ = 98.3 Hz	P _c δ = 72.80	n.a.	P _a δ = 67.00 ppm	$^{2/3}J_{ab}$ = 5.1 Hz
P _{c/d} δ = 62.12 ppm	$^2J_{cd}$ = -9.5 Hz	P _{a,b,c,d} δ = 63.40		P _b δ = 69.10 ppm	$^2J_{ac}$ = -21.2 Hz
P _e δ = 87.25 ppm	$^{2/3}J_{ab}$ = -4.9 Hz			P _c δ = 72.30 ppm	$^2J_{ad}$ = -22.0 Hz
	$^2J_{ac/bd}$ = -18.6 Hz			P _d δ = 61.10 ppm	$^2J_{ae}$ = 106.7 Hz
	$ ^{2/3}J_{ed/ec} $ = 4.7 Hz			P _e δ = 90.94 ppm	$^2J_{bc}$ = 101.6 Hz
	$^2J_{ea/eb}$ = -15.5 Hz				$^2J_{bd}$ = -9.7 Hz
					$^2J_{be}$ = -16.6 Hz
					$^2J_{cd}$ = -13.1 Hz
					$^{2/3}J_{ce}$ = 7.2 Hz
					$^{2/3}J_{de}$ = 1.5 Hz
[Mo(N ₂)(dpepp)(1,2-dppp)] isomer A 3a		[Mo(N ₂)(dpepp)(1,2-dppp)] isomer B 3b			
P _a δ = 62.15 ppm	$^{2/3}J_{ab}$ = -6.6 Hz	P _a δ = 43.17 ppm	$^{2/3}J_{ab}$ = -8.2 Hz		
P _b δ = 58.40 ppm	$^2J_{ac}$ = -21.0 Hz	P _b δ = 77.76 ppm	$^2J_{ac}$ = -22.8 Hz		
P _c δ = 55.90 ppm	$^2J_{ad}$ = 99.2 Hz	P _c δ = 56.60 ppm	$^2J_{ad}$ = 98.7 Hz		
P _d δ = 69.81 ppm	$^2J_{ae}$ = -10.6 Hz	P _d δ = 72.50 ppm	$^2J_{ae}$ = -10.8 Hz		
P _e δ = 71.90 ppm	$^2J_{bc}$ = 98.0 Hz	P _e δ = 71.02 ppm	$^2J_{bc}$ = 100.3 Hz		
	$^2J_{bd}$ = -25.1 Hz		$^2J_{bd}$ = -24.4 Hz		
	$^2J_{be}$ = -15.1 Hz		$^2J_{be}$ = -15.8 Hz		
	$^2J_{cd}$ = -4.1 Hz		$^2J_{cd}$ = -3.2 Hz		
	$^{2/3}J_{ce}$ = 1.5 Hz		$^{2/3}J_{ce}$ = 1.5 Hz		
	$^{2/3}J_{de}$ = -1.5 Hz		$^{2/3}J_{de}$ = -1.5 Hz		

Scheme 1

[Mo(N₂)(dpepp)(depe)] (1). As evident from Figures 2 and 3, the complex [Mo(N₂)(dpepp)(depe)] (**1**) exhibits the IR and Raman spectra with the sharpest vibrational features. This agrees with the ^{31}P NMR spectroscopic result that **1** exists in only one isomeric form (see below). The N–N stretch frequency is located at 1952 cm⁻¹ in the IR spectrum and at 1949 cm⁻¹ in the Raman spectrum (Table 1). The position of the metal–N stretch can be inferred from a comparison with the vibrational spectra of [Mo(N₂)(dpepp)(dppm)]. From that comparison, it also becomes clear that the peaks at 527, 523, and 522 cm⁻¹ in the Raman spectra of **1**, **2**, and **3**, respectively (Figure 3), are *not* associated with the metal–N stretching vibrations because

in [Mo(N₂)(dpepp)(dppm)] there is a corresponding peak (at 526 cm⁻¹) which does not shift upon ^{15}N substitution. For the latter complex, $\nu(\text{Mo}–\text{N})$ was rather shown to be located at 453 cm⁻¹.⁹ At the same position there is a (split) peak in the Raman spectrum of **1** which has a counterpart of weak intensity in the IR spectrum (Supporting Information, Figure S1). This intensity difference is characteristic of metal–N stretching vibrations in dinitrogen complexes and has been employed to distinguish between metal–stretching and metal–bending vibrations.¹² The $\delta(\text{Mo}–\text{N}–\text{N})$ vibrations are more difficult to identify. By comparison with the spectrum of [Mo(N₂)(dpepp)(dppm)] they should be located around 500 cm⁻¹. In this spectral region complex **1** exhibits compara-

tively weak IR bands (at 499 and 493 cm⁻¹, cf. Figure 2) which render a definite assignment difficult. Nevertheless, these features are much more intense for compounds **2** and **3** and in these systems can be attributed to $\delta(\text{Mo}-\text{N}-\text{N})$ (see below).

The measured ³¹P NMR spectrum of **1** (Figure 4a top) shows a typical AMM'XX'-pattern. The signal at 48.80 ppm is assigned to the phosphorus atoms P_a and P_b (cf. Figure 1), the signal at 62.12 ppm is associated with P_c and P_d, and the signal at 87.25 ppm belongs to P_e. The simulated spectrum (Figure 4a bottom) was obtained by an analysis of the M- and the X-half-spectra (Figure 4b,c) according to the literature.¹³ Every half-spectrum consists of ten lines (a–j) which in turn are split into doublets because of the coupling with P_e. The coupling constants are obtained by the solution of following equations:

$$N = J_{ac/bd} + J_{ad/bc}; \quad L = J_{ac/bd} - J_{ad/bc}; \quad K = J_{cd} + J_{ab}; \quad M = J_{cd} - J_{ab} \quad (1)$$

The values of *N*, *K*, *L*, and *M* can in turn be obtained from the relations

$$N = a - b; \quad L = \sqrt{(c-f)(d-e)} = \sqrt{(g-j)(h-i)}; \quad K = g - h = i - j; \quad M = c - d = e - f \quad (2)$$

With +98.3 Hz, the *trans*-interactions ²J_{ad/bc} are positive (see below) and cause the largest splitting, as usual. The *cis*-interactions between P_e and the phosphorus atoms of the depe ligand, P_a and P_b, are only transmitted by the metal center; the corresponding coupling constants are negative and have values of ²J_{ea/eb} = −15.5 Hz. This also applies to ²J_{ac/bd} which are −18.6 Hz. The relative signs of the above coupling constants can also be inferred from a comparison with those evaluated for compound **3** by COSY-45 measurements (cf. Scheme 1). The coupling constant between P_a and P_b is due to two interactions, one transmitted by the metal center and one by the ethylene bridge, and has a value of ²J_{ab} = −4.9 Hz. The same applies to the coupling constants between P_c/P_d and P_e. In this case, however, the sign cannot be inferred from a comparison with **3** as the corresponding coupling constants are very small and thus |²J_{ed/ec}| = 4.7 Hz. The remaining *cis*-interaction, ²J_{cd}, is small and negative (−9.5 Hz). Note that this coupling constant results from a metal-mediated interaction and another interaction via P_e which obviously acts to decrease the absolute value of the coupling constant (this is even more pronounced in **3a** and **3b**; see below).

[Mo(N₂)(dpepp)(dppe)] (2). This complex was obtained in two isomeric forms (cf. Figure 1), as evident from the IR spectrum which exhibits two clearly distinct bands for the N–N stretch $\nu(\text{NN})$ at 2007 and 1953 cm⁻¹ (Figure 2). In the Raman spectrum (Figure 3) the corresponding vibrations appear at 2020 and 1960 cm⁻¹. In the region of the metal–ligand vibrations of **2**, two IR-active vibrations can be identified below 524 cm⁻¹, at 507 cm⁻¹ and at 497 cm⁻¹. These bands are attributed to the metal–N–N bending

vibrations $\delta(\text{MoNN})$ (vide supra). On the basis of the IR and Raman spectroscopic information available for the lower-energy region, however, no metal–N stretching vibration can be assigned with safety.

In agreement with the vibrational data, the ³¹P NMR spectrum of [Mo(N₂)(dpepp)(dppe)] (Figure 5, center) reveals the presence of two isomers which can be separated by COSY-45 (cf. Supporting Information, Figure S2). The AA'BB'M spectrum of the first isomer (compound **2a**; Figure 5 top) consists of two groups of signals at 73.80 ppm and 63.40 ppm with an intensity ratio of 1:4. The signal at 73.80 ppm belongs to the axial phosphorus atom, P_e, and the signal at 63.40 ppm is caused by the four phosphorus atoms which are located in the equatorial plane. No coupling constants can be derived from this spectrum with safety. The ³¹P NMR spectrum of the other isomer (*iso*-[Mo(N₂)(dpepp)(dppe)] (**2b**), Figure 5 bottom) exhibits an ABCDE spin system due to five different phosphorus atoms. The signal at 90.94 ppm belongs to the central phosphorus atom of the dpepp ligand, P_e. The COSY-45 spectrum shows an interaction with the signal at 67.00 ppm (P_a) and a large coupling constant (106.7 Hz), indicative of *trans*-coupling. The *cis*-interaction occurs with a coupling constant of ²J = −16.6 Hz to the phosphorus atom P_b which corresponds to the signal at 69.10 ppm. Moreover, there is observable the small *cis*-coupling to P_c. The corresponding coupling constant of ²J = 7.2 Hz is the result of two coupling pathways, one transmitted by the metal center and one by the ethylene bridge. The low value is caused by the opposite signs of these contributions, leading to partial cancelation (vide supra). Because of the same reason, the *cis*-coupling to P_d is very small (1.5 Hz) and can only be detected in the COSY-45 experiment (see below).

The dddd-signal at 72.00 ppm is assigned to the phosphorus atom P_c. The *trans*-coupling to P_b is large (²J = 101.6 Hz). Furthermore, there exist two metal-mediated *cis*-couplings to P_a (²J = −21.2 Hz) and P_d (²J = −13.1 Hz). The signal at 69.10 ppm with a dddd-structure is assigned to the phosphorus atom P_b. Other than the already mentioned couplings, there exist two *cis*-interactions to P_d and P_a with coupling constants of ²J = −9.7 Hz and ²J = 5.1 Hz, respectively. The coupling constants of the signal at 67.0 ppm could not be determined unambiguously. The phosphorus atom P_a which gives rise to this signal couples with four different phosphorus atoms, so theoretically a dddd-structure should result. The fact that a ddt-structure is observed can only be explained if the coupling constants to P_d and P_c have exactly the same value. The corresponding simulation gives a value of ²J = −22.0 Hz. The signal at 61.10 ppm, finally, does not show a large splitting attributable to *trans*-coupling to another phosphine. It is therefore assigned to the phosphorus atom P_d in *trans*-position to the N₂ ligand. For this signal the simulation gives a superposed ddd-structure.

To determine the relative signs of the above coupling constants, a 45° COSY spectrum has been recorded (Supporting Information, Figure S2). Figure 6 shows the crosspeak resulting from the coupling between P_a and P_b. The crosspeak consists of signals arranged in eight squares. Every

(12) Tuczek, F.; Horn, K. H.; Lehnert, N. *Coord. Chem. Rev.* **2003**, *245*, 107–120.

(13) Günther, H. *Angew. Chem.* **1972**, *19*, 907.

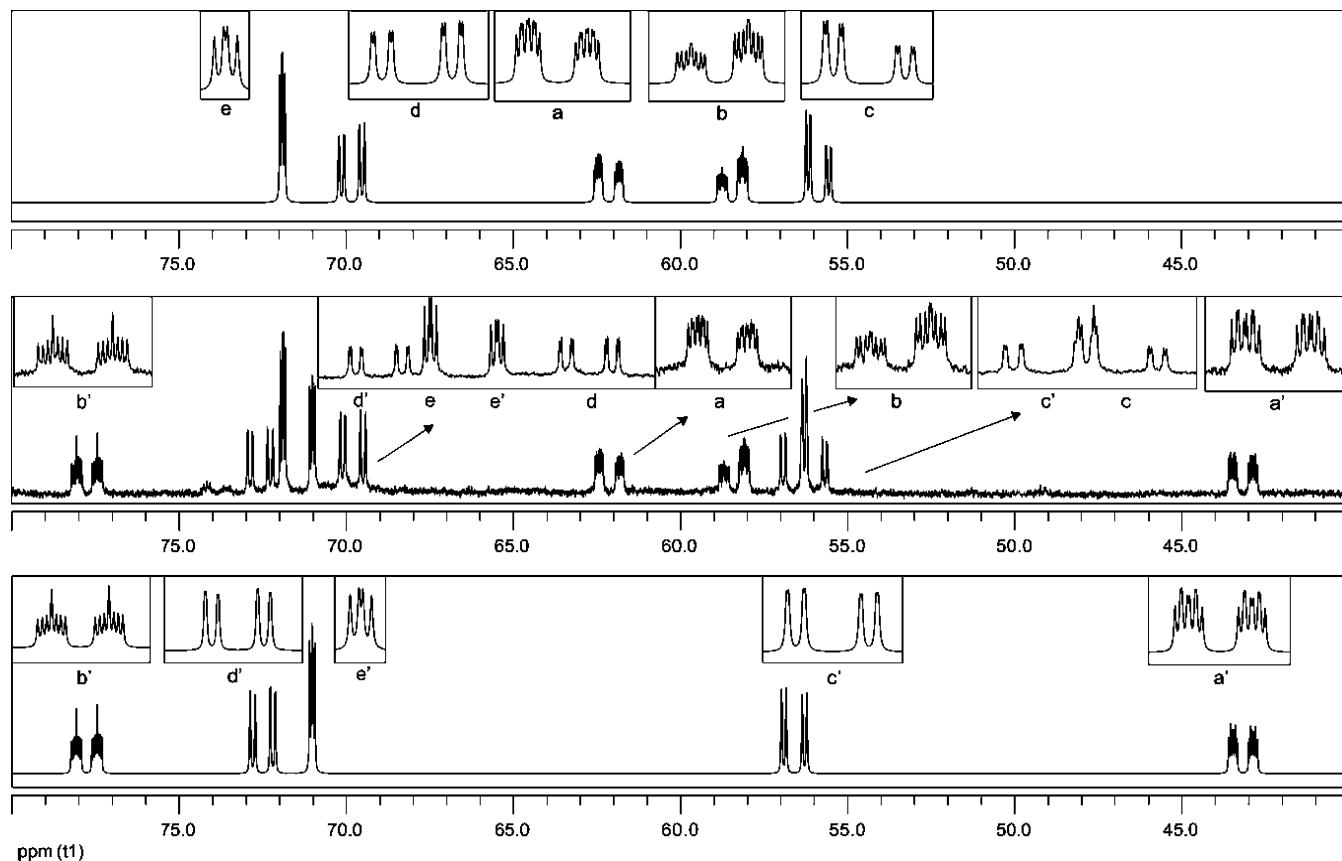


Figure 7. $^{31}\text{P}\{^1\text{H}\}$ -NMR (161.98 MHz, in $\text{THF}-d_8$) of $[\text{Mo}(\text{N}_2)(\text{dpepp})(1,2\text{-dppp})]$ (**3**), simulated isomer **A** (top), measured spectrum (center), and simulated isomer **B** (bottom).

square has the same side length given by the coupling constant J_{ab} . The shifts of the squares against each other result from the couplings of P_a/P_b with the other phosphorus atoms P_c , P_d , and P_e . The couplings of P_a can be determined from the shifts along the x -axis, and the couplings of P_b from those along the y -axis. The relative signs can be obtained by comparison of the shifts due to the coupling with the same phosphorus atom. If both shifts occur toward higher or lower frequency, they have the same sign; if they point into different directions then the signs are opposite (often the vector sum of these shifts is considered, and the “tilt” of the resultant with respect to the x -axis is taken to indicate the relative sign)¹⁴ In the $\text{P}_a\text{--P}_b$ crosspeak, for example, the coupling constants J_{ac} and J_{bc} with phosphorus atom P_c have different signs and the couplings J_{ad} and J_{bd} with P_d have the same sign. All crosspeaks of compound **2b** have been analyzed this way (Supporting Information, Figures S3–S10). If, according to the literature, the value of the *trans*-coupling is assumed to be positive, then the other absolute signs can be derived in relation to this assumption.

$[\text{Mo}(\text{N}_2)(\text{dpepp})(1,2\text{-dppp})]$ (3**).** The product of the synthesis described above contains two isomers **A** and **B** (see Figure 1). This is also reflected by the IR spectrum of $[\text{Mo}(\text{N}_2)(\text{dpepp})(1,2\text{-dppp})]$ (**3**) which shows a broad band at 1957 cm^{-1} for $\nu(\text{NN})$; the same vibration gives a broad peak in the Raman spectrum at 1953 cm^{-1} . Again several shoulders appear in the IR spectrum below 520 cm^{-1} (at 510

and $\sim 500\text{ cm}^{-1}$) which can be assigned to the $\text{Mo}\text{--N}\text{--N}$ bending vibrations. In the lower-energy region, no identification of $\nu(\text{Mo}\text{--N})$ is possible without ^{15}N substitution.

^{31}P NMR spectroscopy was employed to obtain information about the structure of compound **3** in solution. To analyze the spectra and, in particular, to determine the signs of the coupling constants, a COSY-45 spectrum was recorded and analyzed as described for compound **2b** (Supporting Information, Figure S11). On the basis of this information, the signals in the ^{31}P NMR-spectrum of **3** (Figure 7 center) can be assigned to isomers **A** and **B**, both of which are ABCDE spin systems. First, the spectrum of isomer **A** is analyzed (Figure 7, top; cf. Supporting Information, Figures S12–S19). The signal at 71.90 ppm exhibiting a dd-structure is attributed to the phosphorus atom P_e which is coordinated in *trans*-position to the dinitrogen ligand. Two *cis*-couplings are visible, one to P_b with a coupling constant of $^2J = -15.1\text{ Hz}$ and one to P_a with $^2J = -10.6\text{ Hz}$. The coupling with the phosphorus atom P_c can only be evaluated from an analysis of the COSY-45 spectra, leading to a coupling constant of $+1.5\text{ Hz}$. The coupling with P_d corresponds to -1.5 Hz . This indicates that the interactions transmitted by the metal center and the alkyl bridge have the same magnitude and almost exactly cancel each other. The signal at 69.81 ppm with a ddd-structure is caused by the phosphorus atom P_d . The *trans*-interaction to P_a has a coupling constant of $^2J = 99.2\text{ Hz}$, and the *cis*-couplings to P_b and P_c have J -values of -25.1 and -4.1 Hz , respectively.

(14) Fontaine, X. L. R.; Kennedy, J. D.; Shaw, B. L.; Vila José, M. *J. Chem. Soc., Dalton Trans.* **1987**, 2401.

The dddd-signal at 62.2 ppm is associated with P_a . Other than the mentioned interactions, there exist *cis*-interactions with P_b ($^2J = -6.6$ Hz) and P_c ($^2J = -21.0$ Hz). The signal at 58.40 ppm belongs to the phosphorus atom P_b and exhibits a dddd-structure. The *trans*-coupling with P_c has a coupling constant of $^2J = 98.0$ Hz. The ddd-signal of P_c , finally, is located at 55.90 ppm.

The remaining signals are assigned to the other isomer (**B**, Figure 7 bottom; cf. Supporting Information, Figures S20–S28). In particular, the signal at 77.76 ppm with dddd-structure is associated with the phosphorus atom P_b . There exist a large *trans*-coupling ($^2J = 100.3$ Hz) with P_c , two *cis*-interactions with coupling constants of $^2J = -24.4$ Hz (P_d) and $^2J = -15.8$ Hz (P_e) and a *cis*-coupling with P_a ($^2J = -8.2$ Hz). The signal at 72.50 ppm (P_d) is connected with the signal at 43.17 ppm by a *trans*-coupling constant of 98.7 Hz. In addition to the mentioned *cis*-interaction, there exists another *cis*-coupling with $^2J = -3.2$ Hz to P_c . The signal at 71.02 ppm is associated with the phosphorus atom P_e . This atom which is located in *trans*-position to the dinitrogen ligand exhibits four *cis*-couplings, the already mentioned one to P_b and a second one to P_a ($^2J = -10.8$ Hz). The two interactions with P_c and P_d can only be recovered in the COSY-45 spectra, having values of +1.5 and -1.5 Hz, respectively. The signal at 56.60 ppm exhibits a ddd-structure and belongs to P_c . In addition to the couplings to P_b and P_d , there exists an interaction to P_a with a coupling constant of $^2J = -22.8$ Hz. The signal at 43.17 ppm, finally, shows a dddd-structure and is associated with P_a .

In summary, the ^{31}P NMR spectra of isomers **A** and **B** could be fully analyzed and reproduced by simulation. The coupling constants are very similar in both isomers. Moreover, they closely resemble those of the complex $[\text{Mo}(\text{N}_2)(\text{dpepp})(\text{dppm})]$ (Scheme 1) which has been studied previously (signs of coupling constants have been added for this complex where they are evident from a comparison with compound **3**). However, there are important differences in the chemical shifts: Whereas the chemical shifts of the dpepp ligand are very similar for **3a** and **3b**, those of the 1,2-dppp ligand greatly differ. In particular, the splitting between the resonances of P_a and P_b , $\Delta\delta_{ab}$, is comparable for isomer **A** ($\Delta\delta_{ab} = 3.75$ ppm) to that observed for compounds **1** and **2a** ($\Delta\delta_{ab} = 0$) whereas these resonances are one order of magnitude more split for isomer **B** ($\Delta\delta_{ab} = 34.59$ ppm). We attribute this to a geometric distortion of isomer **B** which is caused by an interaction between the phenyl substituent of the phosphorus atom P_e in *trans*-position of dinitrogen and the methyl group of the 1,2-dppp ligand. Note that this methyl group is directed toward the P_e phenyl group in isomer **B** whereas it points in the opposite direction for isomer **A** and in this case does not interact with the phenyl group of P_e . These considerations suggest that the ^{31}P NMR spectrum with the small splitting between P_a and P_b is associated with structure **3a**, and the isomer with the large splitting between P_a and P_b (isomer **B**) belongs to structure **3b** in Figure 1.

4. Discussion

In the preceding sections ^{31}P NMR and vibrational spectroscopic investigations of Mo dinitrogen complexes with five phosphorus ligands have been presented. This coordination environment has been generated by a combination of a triphosphine (dpepp) and different diphosphine ligands with C_2 bridges (depe, dppe, and 1,2-dppp). The structure and bonding of this type of complexes has been described in detail in reference 9. The emphasis of the present paper lies on the NMR-spectroscopic characterization of these complexes, in particular, on the spectroscopic identification of different isomers in solution. This issue is of key relevance whenever the synthesis of a catalytically active complex with predefined properties on the basis of multidentate coligands is pursued.

The ^{31}P spectra of the title compounds were fully analyzed and reproduced by simulation, leading to the identification of one isomer for the complex $[\text{Mo}(\text{N}_2)(\text{dpepp})(\text{depe})]$ (**1**). In contrast, two isomeric forms were evidenced for compound **2**, $[\text{Mo}(\text{N}_2)(\text{dpepp})(\text{dppe})]$ **2a** and *iso*- $[\text{Mo}(\text{N}_2)(\text{dpepp})(\text{dppe})]$ (**2b**), as well as compound **3**, $[\text{Mo}(\text{N}_2)(\text{dpepp})(1,2\text{-dppp})]$ (isomers **A** and **B**). For the latter complex, the methyl group of the 1,2-dppp ligand either points into the direction of the N_2 ligand (**3a**) or into the opposite direction (**3b**). These results were found to be compatible with the corresponding vibrational (IR and Raman) data, showing an unsplit N–N stretch for **1**, strongly split N–N stretching vibrations for compound **2**, and weakly split N–N stretches for compound **3**.

The frequencies of the N–N stretching vibrations (1952 cm^{-1} for **1**, 1953 cm^{-1} for **2a**, 2007 cm^{-1} for **2b**, and 1957 cm^{-1} for **3a/b**) reflect the different degrees of activation imparted to the dinitrogen ligand by the phosphine coligands. Compounds **1**, **3a**, and **3b** have dinitrogen ligands in *trans*-position to the *central* phosphorus atom of the dpepp ligand. All of these complexes exhibit the N–N stretch at $1950\text{--}1960\text{ cm}^{-1}$. The same applies to compound **2a**. Compound **2b**, in contrast, has a *terminal* phosphine group of the dpepp ligand coordinated in *trans*-position to the N_2 ligand. Correspondingly, the N_2 stretch is observed at higher frequency than in **1**, **3a**, **3b**, and **2a**, that is, at $2010\text{--}2020\text{ cm}^{-1}$. This demonstrates the *lower* activation of N_2 in a complex with a *trans*-diphenylalkyl- compared to a complex with a *trans*-dialkylphenylphosphine group. As expected, a much smaller difference in $\nu(\text{NN})$ is observed between the two isomers of $[\text{Mo}(\text{N}_2)(\text{dpepp})(\text{dppe})]$ (**3a** and **3b**) in which the methyl group of the equatorial 1,2-dppp ligand points into different directions (Figure 1).

The ^{31}P NMR spectra of all compounds could be analyzed and perfectly reproduced by simulation, giving a complete set of chemical shifts and coupling constants. A consistent set of coupling constants and corresponding signs was derived for compounds **1–3** and the related complex $[\text{Mo}(\text{N}_2)(\text{dpepp})(\text{dppm})]$ which has been studied previously (Scheme 1). The ^{31}P NMR *trans*-coupling constants were found to be in the range of ~ 100 Hz. For *cis*-coupling, two cases have to be distinguished: If the interaction exclusively

occurs via the metal, the coupling constant is ~ 20 Hz and negative. If the interaction occurs simultaneously over the metal center and an ethylene bridge, the coupling constant is small (sometimes in the order of the line width), indicating that the corresponding coupling pathways correspond to coupling constants with almost identical absolute values but opposite signs. This is in agreement with literature data indicating that the 2J coupling constant via a metal has a negative sign,¹⁵ and the 3J coupling constant via an ethylene bridge a positive sign.¹⁶ It is also known that for second and third-row metals $^2J(\text{P,P})$ *trans*-coupling constants are large and positive.^{17,18} This in turn has been used to determine the absolute signs of coupling constants for compounds **2** and **3**.

The ^{31}P spectra also sensitively reflect the symmetry of the complexes. Quasi-tetragonal symmetry is exhibited by complex **2a** which has one phosphine group in axial and four diphenylphosphine endgroups in equatorial position. The signals deriving from the equatorial phosphines a,b,c,d appear almost unsplit. A similar geometry is present in compound **1**. However, in this case the equatorial diethylphosphine and diphenylphosphine groups P_a/P_b and P_c/P_d , respectively, appear at different chemical shifts (48.80 and 62.12 ppm, respectively). Diethylphosphine is a stronger σ -donor than diphenylphosphine and the latter is a stronger π -acceptor than diethylphosphine; P_a and P_b are therefore more shielded than P_c and P_d . In compound **3**, finally, the symmetry of complex **2a** is broken by an additional methyl group attached to the ethylene bridge of the equatorial diphos ligand. The methyl group can point “upward” (i.e., in the direction of the N_2 ligand; isomer **3a**) or “downward” (i.e., in the opposite direction; isomer **3b**). Importantly, isomer **B** exhibits a significantly larger splitting between the ^{31}P resonances of the bidentate ligand than found for the corresponding depe and dppe complexes. This is attributed to a distortion of the complex because of a steric interaction between the additional methyl group of the diphosphine and the phenyl group of the phosphorus atom P_e in *trans*-position to the N_2 ligand and correlates isomer **B** with structure **3b**. Correspondingly, isomer **A** is correlated with structure **3a** of Figure 1.

For complex **2** an *iso*-form (**2b**) has been identified in which the central phosphorus atom of the dpepp ligand is in equatorial position; that is, *cis* to the dinitrogen group. From

the relative intensities in the ^{31}P NMR spectrum **2a** and **2b** occur in about equal amounts. Astonishingly, however, no corresponding *iso*-forms could be evidenced for compounds **1** and **3**. For the depe complex **1** this may have *electronic* reasons; that is, a configuration where the diethylphosphine groups are in *trans*-position to diphenylphosphine groups may be particularly favorable as strongly electron-donating groups are arranged in *trans*-position to strongly electron-accepting groups. For the 1,2-dppp complex **3**, on the other hand, *steric* reasons may account for the lack of the *iso*-form. Specifically, for **3b** (with the methyl group pointing downward) an *iso*-form may be unfavorable as in *trans*-position of the dinitrogen ligand there would be two phenyl groups instead of one coming in close contact with the methyl group. For **3a**, on the other hand, this argument would not apply, and no principal reasons are visible which would prevent the formation of an *iso*-form in this geometry.

To conclude, the vibrational and ^{31}P NMR spectroscopic properties of three complexes with five coordinating phosphine groups have been determined, and correlations between their geometries and their spectroscopic properties have been derived. In a previous paper it has been shown that the activation of N_2 in these complexes is higher than in corresponding bis(diphosphine) complexes with two dinitrogen ligands but lower than in *trans*-acetonitrile dinitrogen complexes with two diphosphine coligands.⁹ The latter systems, on the other hand, have the disadvantage that the nitrile coligands are labile. As dinitrogen complexes with a pentaphosphine ligation have also been shown to be protonatable at the N_2 ligand,⁸ these systems appear to represent a good compromise between sufficient activation of the dinitrogen ligand on the one hand and thermodynamic/kinetic stability of the ligand environment on the other. This agrees with our theoretical finding that a catalytic cycle of ammonia synthesis on the basis of a Mo pentaphosphine complex should be feasible.¹⁰ Practically this concept is limited by the fact that the phosphine ligand in *trans*-position of N_2 gets labile at higher oxidation states of the metal (e.g., in the nitrido complex) and sooner or later will be replaced by another Lewis-basic ligand or a solvent molecule. Therefore, the necessity persists to covalently attach the *trans*-ligand to the complex in a way that it cannot dissociate at any stage of the catalytic cycle. Concepts to achieve such an architecture on the basis of phosphine ligands for an efficient homogeneous catalyst of ammonia synthesis have been developed and are continued to be actively pursued in our group.¹⁹

Acknowledgment. Support of this research by DFG Tu58-12-2 (SPP1118 “Sekundäre Wechselwirkungen”) is gratefully acknowledged.

Supporting Information Available: IR, Raman, and COSY-45 spectra of the compounds (PDF). This material is available free of charge via the Internet at <http://pubs.acs.org>.

IC800389G

- (15) Pregosin, P. S.; Kunz, R. W. *NMR Basic Principles and Progress. ^{31}P and ^{13}C NMR of Transition Metal Phosphine Complexes*; Springer-Verlag: New York, 1979.
- (16) Friebohn, H. *Ein- und zweidimensionale NMR-Spektroskopie*; Wiley VCH: Weinheim, 2006.
- (17) (a) Bertrand, R. D.; Ogilvie, F. B.; Verkade, J. G. *J. Am. Chem. Soc.* **1970**, *92*, 1916. (b) Ogilvie, F. B.; Jenkins, J. M.; Verkade, J. G. *J. Am. Chem. Soc.*, **1970**, *92*, 1908. (c) Crumbliss, A. L.; Topping, R. J. *Phosphorus-31 NMR: Spectral Properties in Compound Characterization and Structural Analysis*; VCH: New York, 1987; Vol. 15. (d) Hughes, A. N. *Phosphorus-31 NMR: Spectral Properties in Compound Characterization and Structural Analysis*; VCH: New York, 1987; Vol. 19. (e) Clark, H. C.; Kapoor, P. N.; McMahon, I. J. *J. Organomet. Chem.* **1984**, *190*, C101. (f) Airey, A. A.; Swiegers, G. F.; Willis, A. C.; Wild, S. B. *Inorg. Chem.* **1997**, *36*, 1588.
- (18) This does not apply to first-row metals where $^2J(\text{P,P})$ for *trans*-coupling may be negative, cf. ref. 17a. Likewise, $^2J(\text{P,P})_{\text{cis}}$ and $^2J(\text{P,P})_{\text{trans}}$ values for metal complexes in the first transition-metal series can be of similar magnitude whereas in the second and third series the *trans*-coupling is usually much larger.

- (19) Stephan, G.; Näther, C. N.; Sivasankar, C.; Tuczek, F. *Inorg. Chim. Acta* **2008**, *361*, 1008–1019.